ELSEVIER

Polymer 44 (2003) 1425–1435

polymer

www.elsevier.com/locate/polymer

# The Degradation of Polyglycolide in Water and Deuterium Oxide. Part II: Nuclear Reaction Analysis and Magnetic Resonance Imaging of Water Distribution

Georgina E. Milroy[a], Richard W. Smith[b], Rebecca Hollands[b], Anthony S. Clough[b], Michael D. Mantle[c], Lynn F. Gladden[c], Hiep Huatan[d], Ruth E. Cameron[a,*]

[a]*Department of Materials Science and Metallurgy, Cambridge Centre for Medical Materials, University of Cambridge, Pembroke Street, Cambridge CB2 3QZ, UK*

[b]*Department of Physics, School of Electronics & Physical Sciences, University of Surrey, Guildford GU2 7XH, UK*

[c]*Department of Chemical Engineering, University of Cambridge, Pembroke Street, Cambridge CB2 3RA, UK*

[d]*Pfizer Ltd, Pharmaceutical R&D, Sandwich, Kent CT13 9NJ, UK*

Received 11 June 2002; received in revised form 5 November 2002; accepted 21 November 2002

**Abstract**

Magnetic resonance imaging (MRI) and scanning microbeam nuclear reaction analysis (NRA) were used to monitor changes of water ingress into polyglycolide (PGA) disks with degradation time. MRI detects $H_2O$, whereas NRA is sensitive to $D_2O$. The acid-catalysed hydrolysis of the ester is significantly slower in $D_2O$ than $H_2O$ because of the kinetic isotope effect. This behaviour was investigated in Part I. In this paper, NRA was used to investigate PGA hydration in buffers made from $D_2O$, and NRA and MRI experiments were performed on samples degraded buffers made from a 50% mixture of $D_2O$ and $H_2O$ ($D_2O/H_2O$ 50:50) to allow a comparison between the two techniques. The NRA and MRI results provide direct evidence in support of the four-stage reaction–erosion model reported in previous literature, and show that this model applies to polymer degradation in heavy water and in a buffer made from $D_2O/H_2O$ 50:50. It is believed that this is the first time that NRA and MRI have been compared for the same hydrating system.


*Keywords:* Polyglycolide; Poly(glycolic acid); Magnetic resonance imaging

## 1. Introduction

PGA is a semi-crystalline polyester that degrades by ester hydrolysis over a few weeks. It is currently used in medical implants, for example, sutures, but it has also shown potential as a material for controlled drug delivery. PGA shows few observable changes over the first few days of degradation, followed by significant polymer mass loss, water uptake and drug release [1]. The reaction by-products are acidic and autocatalyse the ester hydrolysis process causing the rate of degradation to be higher in the centre of the polymer than at the surface. This is because, the macromolecular nature of the by-products means they have small diffusion coefficients, and initially only those near the surface migrate into the surrounding medium. The bulk degradation process of the system therefore involves the complex interplay between reaction and diffusion. This behaviour is characteristic of heterogeneous bulk erosion [2].

In previous work, polymer degradation and its correlation with drug release were discussed in terms of a four-stage model [1]. In stage I, low levels of water are absorbed into the sample. In stage II, the molecular weight falls steadily as the absorbed water reacts with the polymer. Insertion secondary crystallisation is thought to take place at this point due to enhanced polymer mobility caused by the falling molecular weight and water plasticisation. At the beginning of stage III, a critical molecular weight is reached and oligomers begin to diffuse from the surface of the sample. This in turn encourages water sorption at the surface and co-operative diffusion of oligomers out of and water

* Corresponding author. Tel.: +44-1223-334324; fax: +44-1223-334567.

*E-mail address:* rec11@cam.ac.uk (R.E. Cameron).

0032-3861/03/$ - see front matter © 2002 Elsevier Science Ltd. All rights reserved.
PII: S0032-3861(02)00884-4

into the sample, giving a fairly sharp reaction–erosion front. Behind this front, the sample is highly hydrated and porous, whilst ahead of the front, oligomers have yet to diffuse out and there is a low water content. It is hypothesised that during stage III, the fronts move towards the centre of the sample. Stage IV is thought to begin when the fronts meet, presumably in the centre. Drug release seems to correlate with the movement of these fronts, beginning significantly at the onset of stage III.

In Part I, it was shown that in the presence of $D_2O$ rather than $H_2O$, the degradation rate of PGA significantly decreased: each stage of degradation started later and lasted for a longer period of time. This observation was made by monitoring long period, polymer mass loss, water uptake, drug release and buffer pH during polymer degradation. The effects observed were due to a kinetic isotope effect [3]. This phenomenon involves a reduction in the rate of C–H bond scission in the presence of deuterium atoms due to a reduction of the zero-point energy of the bond. The size of the change depends on the experimental parameters involved and is determined empirically. In this paper, we use two imaging techniques, nuclear reaction analysis (NRA) (which detects $D_2O$) and magnetic resonance imaging (MRI) (which detects $H_2O$), to monitor water ingress into PGA during degradation and perform a comprehensive study of the hydration behaviour of the polymer in a $D_2O$ buffer, and a buffer made with 50% $D_2O$ and 50% $H_2O$. The results are used to investigate the four-stage degradation model for the polymer. Unlike Part I, this study does not consider the drug release behaviour of the polymer.

Scanning microbeam NRA has proved a very versatile technique for monitoring diffusion in a wide range of systems (for example, surfactants in hair, water diffusion in optic cables) [4–6]. Recently, the technique has successfully given data on water ingress and drug release from polymeric matrices (for example, hydrosilanised silicone polymers, [7]).

The theory of NRA is documented extensively in the literature, and only a brief description is given here [8].

A $^3He^+$ ion beam from a Van de Graaff accelerator is used to bombard a cross-section face of a sample soaked in deuterated water and subsequently frozen in liquid nitrogen. The ion beam induces the following reaction.

$$^3\mathrm{He} + \mathrm{d} \rightarrow \mathrm{p} + \alpha, \qquad Q = 18.4\ \mathrm{MeV} \tag{1}$$

where d is the deuterium nucleus, p, the proton with an energy characteristic of the system, α the $^4$He nucleus and $Q$ is the energy released due to mass changes; $Q = (m_{\mathrm{He}} + m_{\mathrm{d}} - m_{\mathrm{p}} - m_{\alpha})c^2$.

As the beam scans the face of the sample, protons are collected using a 1.5 mm thick silicon surface barrier detector. The proton energy (approximately 12 MeV) is well separated from ions undergoing other interactions such as Rutherford backscattering. The intensity of protons generated at a point in the sample is proportional to the number of deuterated molecules resident at that point. Samples soaked in deuterated conditions for different times can give information about the development of hydration with time in the system. Previous work has shown that the ingress of deuterated media was representative of water ingress in the same system with differences in hydration rate accounted for by the differences in the mass and diffusion rates of H and D atoms [9]. Of course, this is only true if the rate of water ingress is controlled by diffusion processes alone.

MRI is a versatile technique that has provided qualitative and quantitative information about liquid transport in a wide range of polymers [10–14]. It has many advantages over other imaging techniques; for example, it is non-invasive, chemically selective and suitable for in situ experiments. The theory of nuclear magnetic resonance (NMR) is well documented, and the reader is referred to appropriate literature, as only a brief discussion of the theory behind NMR and MRI is presented here [15].

Modern NMR spectroscopy subjects a selected type of nucleus or *spin system* from a material to electromagnetic radiation in the form of radio frequency (RF) pulses when placed in an external magnetic field, $\mathbf{B}_0$. In this study, the spin system was the proton nuclei present in the PGA samples. This action perturbs the distribution of nuclear spins between two energy levels. A NMR signal may then be detected as the equilibrium distribution between the two energy levels is restored via a process known as relaxation.

Relaxation involves the return of two types of magnetisation to equilibrium: longitudinal ($\mathbf{M}_z$) and transverse ($\mathbf{M}_{xy}$). The first process is called spin–lattice or $T_1$ relaxation, and is associated with the rate of energy transfer between the excited spin states and the surrounding lattice of the material. Spin–lattice relaxation is associated purely with the recovery of net magnetisation in the $z$-direction. The second relaxation process is called, spin–spin or $T_2$ relaxation, and concerns how long the transverse magnetisation remains in the $x$–$y$ plane. $T_2$ gives a measure of the relaxation period before $\mathbf{M}_{xy}$ returns irreversibly to the equilibrium value of $\mathbf{M}_z$ ($t = 0$) and thus $T_2 \leq T_1$. For water transport into systems like PGA, knowledge of $T_1$ and $T_2$ values are important in order to determine whether the spatial NMR signal recorded is a quantitative measure of the number of resonant spins present in the sample under study. In general, quantitative NMR measurements are only possible when the $T_1$ and $T_2$ relaxation behaviour of the system is known.

Spatial resolution of the NMR signal to give two-dimensional data involves the application of additional smaller magnetic field gradients (usually in the $x$, $y$ and $z$ laboratory directions) to the main field $\mathbf{B}_0$ [15]. Magnetic field gradients and RF excitation pulses can then be combined to produce one, two or three-dimensional maps showing the spatial distribution of a molecular species.

In this paper, we present NRA data for PGA degradation

in pure $D_2O$ and discuss the results in the context of the four-stage degradation model. In addition, we present and compare data from NRA and MRI for PGA degradation in a buffer containing a 50:50 mixture of $D_2O$ and $H_2O$. This will include plotting the distance moved by water fronts against time from NRA and MRI one-dimensional profiles.

## 2. Experimental

### 2.1. Sample preparation

Samples were made according to the method described by Hurrell et al., which gave them uniform and controlled thickness [1]. A PGA batch was obtained in powder form from Alkermes Medisorb Polymer, Ohio, USA, which had an intrinsic viscosity of 1.3 dl/g. Samples were processed into disks of diameter 15 and 2.3 mm thickness using a mould on a hot press. Samples prepared in this way are more uniform in thickness than the samples prepared using the method reported in Part I. The mould consisted of a top and base made from PTFE coated aluminium, and an aluminium or steel spacer of chosen thickness with circular holes forming the mould cavity. The base and spacer of the mould was placed on the heated lower plate of a Magnus compressible hot press. The temperature varied across the face of the press and a thermocouple was used to calibrate the press before and after use. The mould was filled with PGA powder in stages to ensure that the mould fully filled. Between each stage, the lower and upper plates of the press were brought almost into contact for approximately 1 min to allow the polymer to melt before more polymer was added if required. Once the mould was filled, the second PTFE coated aluminium foil was placed over the polymer. A pressure of 10 bar at 236 °C was then applied, for approximately 30 s. The mould and polymer were then removed immediately to iced water. Samples showed a slight rippling on the surface.

Samples were degraded, without agitation, at 37 °C in phosphate buffered saline (with a mass equivalent to the volume of PBS made using 100% $H_2O$), with pH 7.4 and concentration 0.01 M. For MRI, the solvent used was a 50:50 mixture of $D_2O$ and $H_2O$, and for NRA, the solvent used was either pure $D_2O$ or a 50:50 mixture of $D_2O$ and $H_2O$. The disks were supported in perspex grooves to expose them to the buffer, and the solutions and bottles were autoclaved at 120 °C and 1 bar for 30 min before use.

### 2.2. Scanning microbeam nuclear reaction analysis (NRA)

NRA was conducted at the University of Surrey using a 2 MeV Van de Graaff accelerator. A 1.1 MeV $^3He^+$ ion beam, with an approximate current of 5 nA, was produced and directed along an evacuated beam line leading to the sample. The beam was focused using four magnetic quadrapole lenses to a spot of diameter 40 μm on the sample face from an initial circular aperture of diameter 200 μm. The beam was raster-scanned across the sample face by computer controlled crossed electric fields.

Samples were cooled in liquid nitrogen to freeze the water profile and minimise sample drying, and then cleaved in half. The newly formed surfaces were smoothed using a razor blade directed along the length of the disk diameter (perpendicular to the water front movement direction). This procedure was difficult to conduct when samples had undergone either very little degradation, because they were very hard, or significant degradation, because they were very soft and prone to cracking. Consequently, nearly all the cleaved surfaces exhibited quite a rough topography that introduced scatter to resulting data.

The samples were then placed between two copper blocks mounted on an aluminium plate, and placed on a liquid nitrogen-cooled sample copper-base plate inside the target chamber and evacuated to $10^{-6}$ Torr. Computer controlled crossed electric fields were used to raster scan the beam over the sample surface. The beam was scanned across a region in the centre of the sample face to avoid edge effects from water diffusing into the sample from the sides as well as the top and bottom faces of the disk. The run time was approximately 15 min. The computer correlated the number of detected protons with the scan position of the ion beam to give two-dimensional maps showing the variation of resident deuterium across the sample. The equipment was calibrated using deuterated polystyrene.

The raw data was initially normalised by dividing the number of proton counts from the sample by the number of backscatters per unit area recorded for the copper blocks. However, the normalisation factors were then scaled using water gain results determined gravimetrically, because initial results showed that the samples had dried at the surface as they were mounted on the copper blocks even though they had been cooled in liquid nitrogen.

To obtain one-dimensional data, three random slices were selected from the two-dimensional scan (each 10 pixels in width) and used to determine the mean profiles.

### 2.3. Magnetic resonance imaging (MRI)

Two-dimensional spin density MRI was used to record the water ingress into polyglycolide disks in the $x-z$ plane. A standard spin-echo pulse sequence was used. A 90° Gaussian-shaped selective RF excitation pulse was applied to the sample in the presence of the $\mathbf{G}_y$ (slice) magnetic field gradient. Classically, this causes the net magnetisation, $\mathbf{M}_z$, within the selected slice to rotate by 90° from the $z$-direction into the to the $x-y$ plane. This transverse magnetisation was then further frequency and phase encoded by the application of two orthogonal magnetic field gradients in the $x$ and $z$ directions, respectively. After applying a refocusing 180° selective RF pulse, the signal was then acquired in the presence of a second frequency encoding gradient yielding typically '$n$' data points. The whole process was then

repeated for '$m$' different value of the phase encoding gradient until enough data points are acquired to build up a spin density image, typically yielding an image of $n$ by $m$ data points. Two-dimensional Fourier transformation of the frequency-phase encoded data set then yielded a two-dimensional spin-density map or image in the $x-z$ plane of the disk.

One-dimensional data were obtained by extracting individual profiles in the phase encoding direction (here in the $z$-direction). An average of three individual profiles were used to obtain a mean one-dimensional profile.

All MRI experiments were conducted using a Bruker DMX 300 NMR spectrometer corresponding to a proton resonance frequency of 300.13 MHz. PGA samples were placed on a perspex support, put in a glass tube, and then placed into the $\mathbf{B}_0$ external field and imaged individually. The samples were covered with cling film to minimise water loss due to drying. A series of disks were tested, each degraded for a different time, and gave data corresponding to an individual time-point. A microimaging probe-head was used to obtain $^1$H images of 128 by 64 pixels. Spatial resolution was obtained with shielded magnetic field gradients of 15.98 G/cm in the $\mathbf{G}_z$ and $\mathbf{G}_x$ directions, and 10.79 G/cm for the $\mathbf{G}_y$ slice gradient. The field of view was approximately 20 mm by 6 mm in the $x-z$ plane, and the pixel resolution was therefore approximately 156 μm by 94 μm. The $x-z$ slice thickness was 1.5 mm. A data acquisition time of 25 min was used to achieve an acceptable signal-to-noise ratio. An echo time (TE) and recycle time (TR) of 2.9 ms and 3 s were used, respectively.

For the experimental conditions used here, MRI was not sensitive enough to measure the low levels of water present over the first 21 days of the degradation process.

Tests were also performed on samples which were degraded in 100% $D_2O$ 0.01 M PBS for 46 days to determine if any signal was produced due to species other than $H_2O$, such as the mobilisation of the polymer. The result suggested that only $H_2O$ in the polymer contributed to a MRI signal.

Relaxation time ($T_1$ and $T_2$) and self-diffusion weighting will influence the signal intensity obtained in the MRI data. The expected signal loss from self-diffusion weighting is calculated to be less that 0.02% and has therefore been considered negligible in this analysis. However, relaxation-time contrast within the images is significant and has been considered in detail elsewhere [16]. In summary, the $T_1$ relaxation losses associated with $H_2O$/PGA system varied between 3.6% for 21 days degradation and 15.3% for 41 days degradation. Signal intensity losses due to $T_2$ are more severe and are estimated to lie in the range 19–40%. The MRI data were used to obtain (i) the position of the penetrant front, and (ii) and estimate of liquid content within the polymer. The images were acquired using the minimum echo time, thus minimising $T_2$ contrast for this system and maximising the ability to detect the presence of liquid in the polymer. Thus, the position of the penetrant front, i.e. the position at which the first detectable liquid signal is obtained is acquired as accurately as possible. The detailed shape of the penetrant front will be sensitive to local relaxation time contrast effects, which are not corrected for and hence the shape is not considered quantitative. The estimation of liquid uptake is provided by normalising the average signal intensity obtained for a PGA sample which has undergone degradation over a period of 35 days to the gravimetric measure of liquid uptake in that sample. This sample was chosen as it contained the full range of $T_2$ values within it. The liquid mass uptake, and hence percentage mass change, associated with other degradation times is obtained by applying this normalisation factor to the average signal intensity value of each set of profiles. Remarkably good agreement between percentage mass uptake obtained by gravimetric measurements, and the MRI data is achieved. It is therefore reasonable to assume that the loss in $^1$H signal intensity in the profiles due to $T_2$ (and $T_1$) relaxation is approximately constant. There is no reason why this argument should not be applied to the $D_2O/H_2O$/PGA system, as the underlying physics of polymer degradation is likely to be the same.

### 2.4. Mass loss and water uptake

The gravimetric method used in this study to determine the water gain and mass loss of PGA samples during degradation was detailed in Part I.

## 3. Results

Fig. 1 shows the mass loss and water gain profiles for 2.3 mm PGA disks degraded in either $H_2O$, $D_2O/H_2O$ 50:50 or $D_2O$ based PBS. The profiles show the relative rates of polymer degradation with varying amounts of $D_2O$ in PBS. Slower changes in mass loss and water gain were observed with increasing amounts of $D_2O$.

Fig. 2 shows the one-dimensional NRA data for PGA

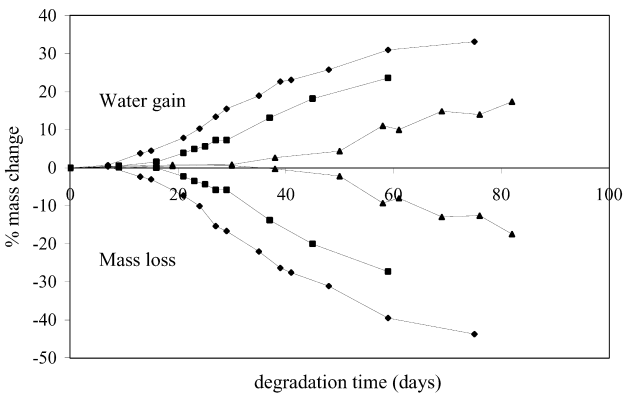


Fig. 1. Percentage mass loss and water content for samples degraded in $H_2O$ (diamonds), $D_2O/H_2O$ 50:50 (squares) and $D_2O$ (triangles). The experimental error in the percentage mass change is ± 1.0 for both pure $H_2O$ and $H_2O/D_2O$ 50:50 and ± 0.4 for pure $D_2O$.

disks degraded in 100% $D_2O$, and recorded for degradation times up to the start of stage III. All results are plotted on the same scale. The figure shows that the water levels remain low and increase slowly up to 29 days, after which, ingress becomes more substantial.

Fig. 3 shows the one-dimensional NRA data for PGA disks degraded in $D_2O$, and recorded for the same degradation times featured in Fig. 2, and also for times after the start of stage III. The scale of the *y* axis of the one-dimensional profiles is different to those in Fig. 2, to allow the later time points to be visualised. The figure shows more clearly than in Fig. 2 that the water uptake was low up to 29 days, after which it increased more significantly. The rough topography, chips and chipped edges of the cleaved surfaces, particularly at high degrees of degradation are presumably the cause of the high degree of scatter, and some of the low level signal at the edges of some of the samples.

Fig. 4 shows the one-dimensional NRA data for PGA disks degraded in $D_2O/H_2O$ 50:50, and recorded for degradation times up to the start of stage III (which starts at an earlier time than for degradation in $D_2O$). The figure shows that the $D_2O$ levels remained low and increased slowly between 11 and 21 days, after which, ingress became more substantial.

Fig. 5 shows the one-dimensional NRA data for PGA disks degraded in $D_2O/H_2O$ 50:50, and recorded for the same degradation times featured in Fig. 5, and also for

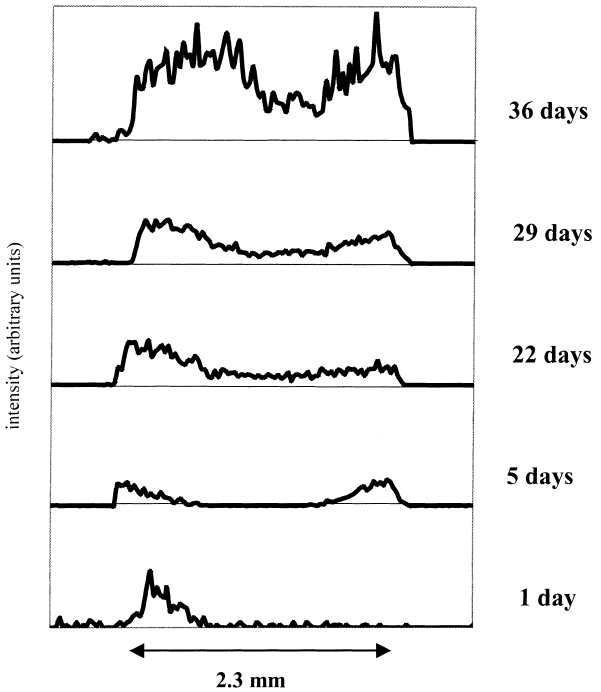


Fig. 2. The mean one-dimensional NRA data for degradation in $D_2O$ show the progress of deuterium into 2.3 mm thick PGA disks for time points from the first 36 days of hydration. All data are plotted on the same vertical scale. The scatter calculated for the area under the one-dimensional profiles is ±8%. The level of scatter in some of the profiles is high perhaps because of the rough surface topography introduced during the cleavage of the samples.

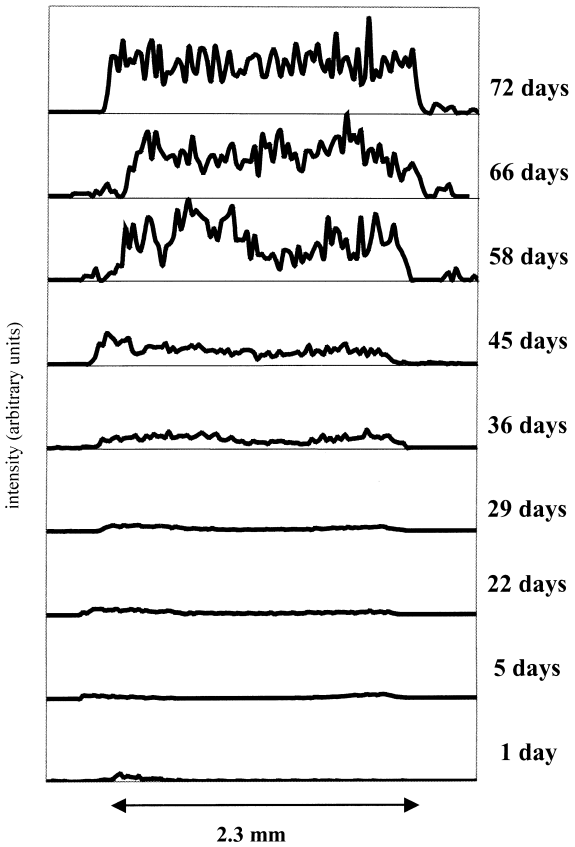


Fig. 3. The mean one-dimensional NRA data for degradation in $D_2O$ show the progress of deuterium into 2.3 mm thick PGA disks with time. All data are plotted on the same scale. The experimental error is calculated for the area under the one-dimensional profiles is ±8%.

times after the start of stage III (which starts at an earlier time than for degradation in $D_2O$). The results show that the water uptake was low up to a time between 11 and 21 days, after which it increases more significantly.

Fig. 6 compares $D_2O$ and $D_2O/H_2O$ 50:50 one-dimensional profiles for selected time points. The data show that PGA degraded more slowly with an increasing fraction of $D_2O$. All data are plotted on the same scale. The level of scatter in the data makes it difficult to compare the distance moved by any water fronts into the polymer from respective profiles.

Fig. 7 shows a plot of the diffusion profile, represented by the counts corresponding to $D_2O$ concentration as a function of distance, the scale of distance given in pixels as measured, obtained from NRA one-dimensional data for 3 days degradation of PGA in $D_2O/H_2O$ 50:50. The best-fit plot is a solution to the error function in equation [3], discussed in Section 4.

Fig. 8 shows a plot of the diffusion profile obtained from NRA one-dimensional data for 5 days degradation of PGA in $D_2O$. The best-fit plot is a solution to the error function in equation discussed in Section 4 [3].

Fig. 9 shows one and two-dimensional MRI data for PGA disks degraded in $D_2O/H_2O$ 50:50 for different degradation

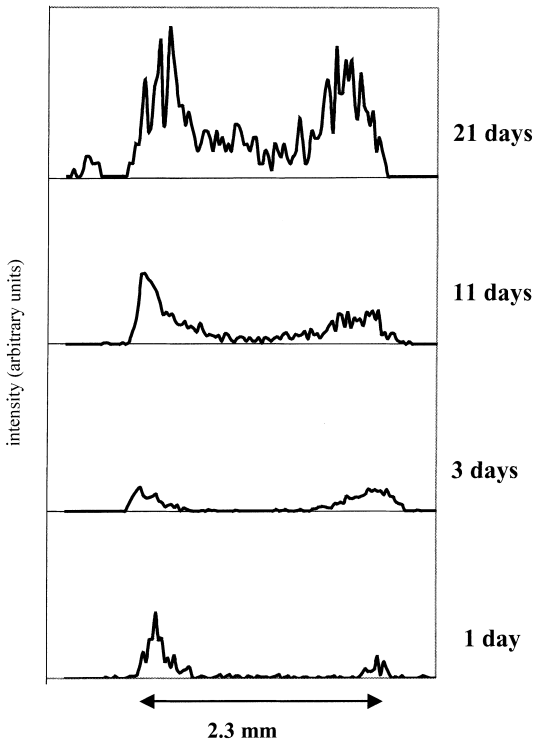


Fig. 4. The mean one-dimensional NRA data for degradation in $H_2O/D_2O$ 50:50 show the progress of deuterium into 2.3 mm thick PGA disks for the first 21 days of hydration. The shapes of the profiles up to 11 days degradation appear to show Fickian diffusion. All data are plotted on the same scale. The experimental error is calculated for the area under the one-dimensional profiles is ±7%.

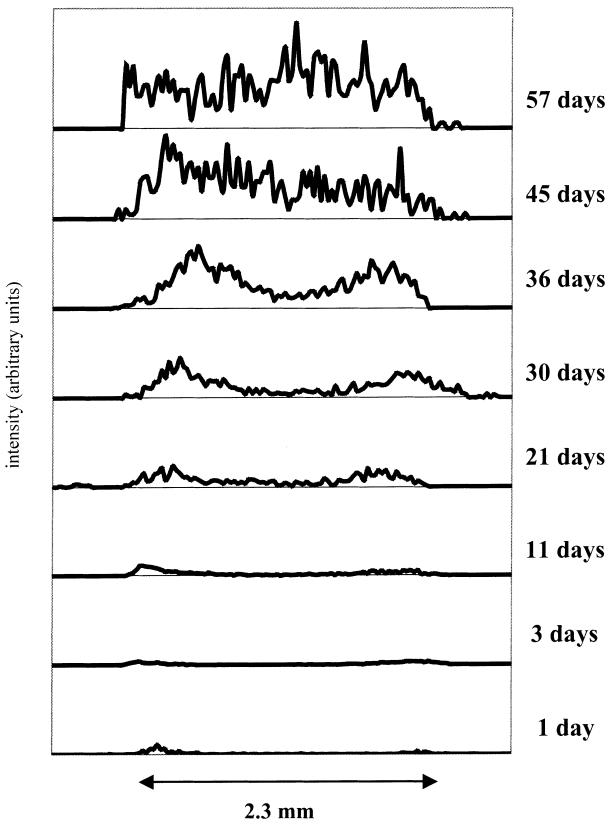


Fig. 5. The mean one-dimensional NRA data for degradation in $D_2O/H_2O$ 50:50 show the progress of deuterium into 2.3 mm thick PGA disks with time. All data are plotted on the same scale. The experimental error is calculated for the area under the one-dimensional profiles is ±7%.

times. All samples measured were in either stage III or stage IV of degradation. The one-dimensional profile for 21 days degradation only shows one distinct peak, and all the profiles show that more water entered from one side of the disk compared with the other. The data show water ingressed as moderately sharp fronts from 21 days onwards, until they meet in the centre just after 47 days. Afterwards, the water ingress continued, and by 75 days, the water distribution was largely homogeneous.

Fig. 10 shows the mass change caused by water gain for PGA samples determined from the MRI data, which is presented alongside equivalent results determined gravimetrically. For the former, each time point was determined by calculating the area under the one-dimensional profiles using Simpson's rule [17], and then converting the value to a percentage mass change by using the value of water gain determined gravimetrically for 37 days (the degradation time when the size of the magnetisation losses due to $T_1$ and $T_2$ relaxation is thought to be represent a mean average of the losses in the MRI signal for PGA degradation in $D_2O/H_2O$ 50:50 [18]). Both data sets agree with each other within experimental error, and both show significant water uptake occurred after about 13 days degradation.

Fig. 11 shows the distance moved by water fronts against time, for degradation in $D_2O/H_2O$ 50:50, determined from MRI and NRA data. Values for the penetration distances were obtained by measuring the mean width of the water fronts from profiles in pixels showing them before they meet. These values were converted to units of distance by equating the width across a profile to the thickness of the sample. For NRA data, the low-level residual water acquired during stages I and II of degradation was subtracted from the one-dimensional profiles before the distance moved by the fronts is calculated. Both data sets predict a linear relationship, and suggest that the reaction–erosion fronts started at about 10(±2) days, and proceeded at a rate of 0.028(±0.004) mm/day into the sample until they met in the centre.

## 4. Discussion

The water gain and mass loss data shown in Fig. 1 indicate clearly that PGA degradation becomes slower with increasing concentrations of $D_2O$. The data suggest that water uptake and mass loss increased substantially after about 10, 13 and 30 days in pure $H_2O$, $D_2O/H_2O$ 50:50 and pure $D_2O$ PBS respectively. From the degradation model, this time is approximately when stage III starts and the reaction–erosion fronts begin to move inwards from the sample surface. These times change non-linearly with

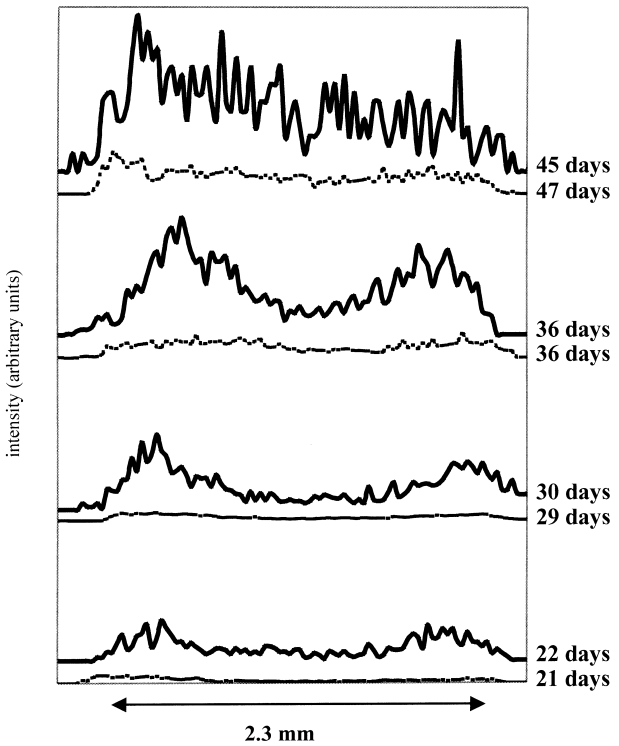


Fig. 6. The mean one-dimensional NRA data for degradation in $D_2O$ (dotted line) and $D_2O/H_2O$ 50:50 (whole line). All data are plotted on the same scale. The experimental error calculated for the area under the one-dimensional profiles is ±8% for $D_2O$ and 7% for $D_2O/H_2O$ 50:50.

increasing amounts of $D_2O$, perhaps because of a non-linearity in the kinetic isotope effect.

The one-dimensional NRA data in Fig. 2 (for fully deuterated buffer) show the levels of $D_2O$ gradually increased with degradation time, with a greater amount of water always residing at the sample edges than the centre. Up to 29 days, the profiles show there was relatively low levels of water, but by 36 days, the levels had started to increase substantially. This behaviour agrees with the data in Fig. 1, which showed little water gain over the first 30

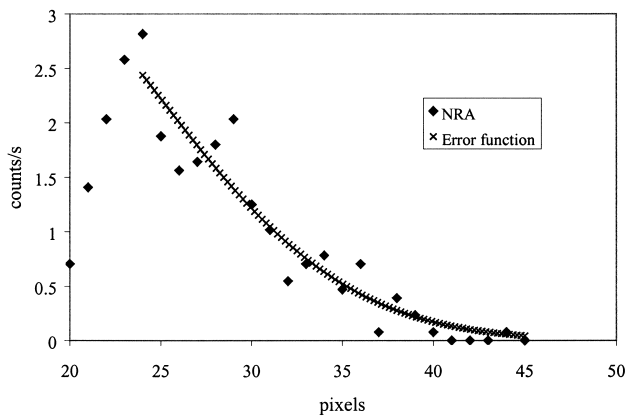


Fig. 7. A plot of the diffusion profile obtained from NRA one-dimensional data for 3 days degradation of PGA in $D_2O/H_2O$ 50:50. The best-fit plot is a solution to the error function in equation [3].

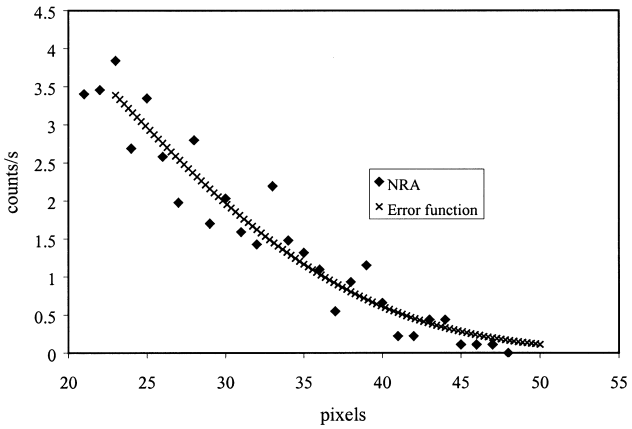


Fig. 8. A plot of the diffusion profile obtained from NRA one-dimensional data for 5 days degradation of PGA in $D_2O$. The best-fit plot is a solution to the error function in equation [3].

days, and a significant increase afterwards for PGA degradation in $D_2O$ PBS.

The NRA data in Fig. 2 provide information about the water ($D_2O$) ingress during stages I and II when the polymer undergoes chain cleavage and a decrease in molecular weight.

The profiles show that water ($D_2O$) seemed to penetrate more from one side of the sample than the other before the fronts have met. This finding has been observed previously in MRI data [18]. It is thought that the bottom side of the polymer is in contact with the press for longer during sample

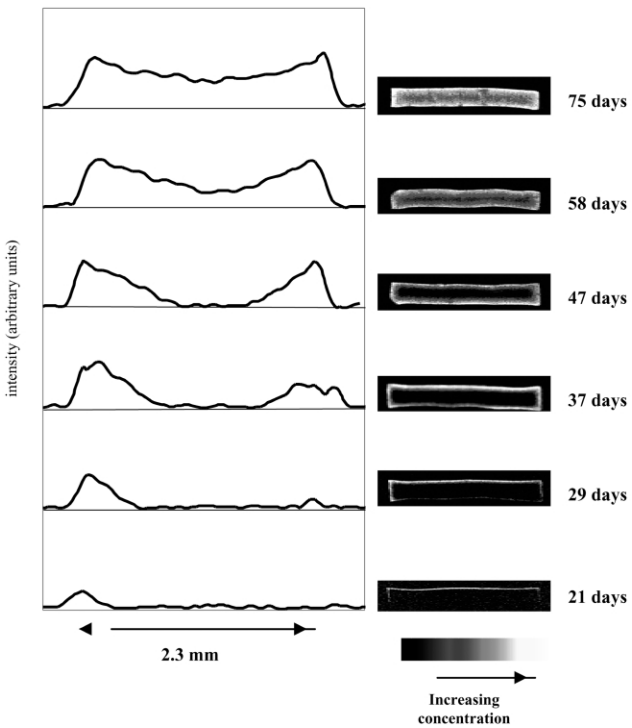


Fig. 9. The mean one and two-dimensional MRI data for degradation in $D_2O/H_2O$ 50:50 show the progress of water into 2.3 mm thick PGA disks with time. All data are plotted on the same scale. The experimental error calculated for the area under the one-dimensional profiles is ±3%.

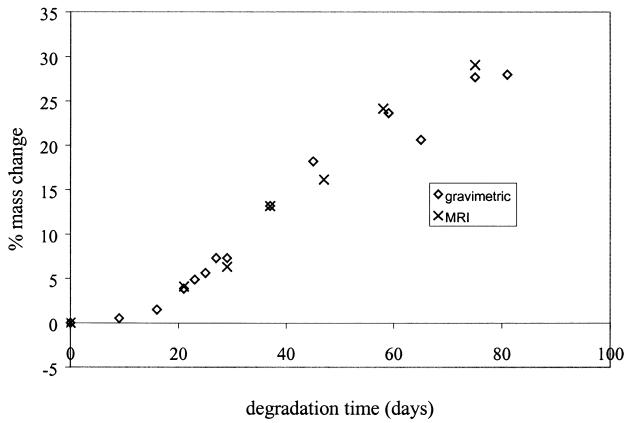


Fig. 10. The percentage mass change due to water gain of 2.3 mm PGA disks degraded in $D_2O/H_2O$ 50:50 determined from gravimetric analysis and MRI one-dimensional profiles. Experimental error is ±1.0% mass change for data determined from gravimetric analysis and ±1.4% mass change for data determined from MRI.

preparation, causing it to undergo more thermal degradation and making the molecular weight lower as a result. This effect would allow hydration and subsequent hydrolytic degradation to occur more easily. GPC results show that after processing, the molecular weight has fallen by a factor of 1.7, which supports this hypothesis [18].

Fig. 3 shows one-dimensional NRA data for PGA degradation in $D_2O$ over a longer period of time than Fig. 2. The figure shows more clearly than Fig. 2 that the level of penetrated water was very low up to 29 days, and increased significantly after 36 days. In addition, the data is consistent with water fronts appearing after 29 days, moving in from the sample surface and meeting in the centre between 58 and 66 days, although the level of noise is very high and no very definite conclusions may be drawn. The results are therefore consistent with the hypothesis that reaction–erosion fronts progress during stage III from the sample surface inwards until they meet in the centre. The level of noise makes the water fronts appear more diffuse when the data are compared to the MRI profiles in Fig. 9.

After 66 days (during stage IV of the degradation model), it appears that water ingress continued, yielding a largely homogenous distribution by 72 days. However, by this stage in the degradation, the polymer was very soft, and samples easily broke-up, proving difficult to test. As a consequence, NRA data cannot give information about PGA hydration after beyond the early part of stage IV.

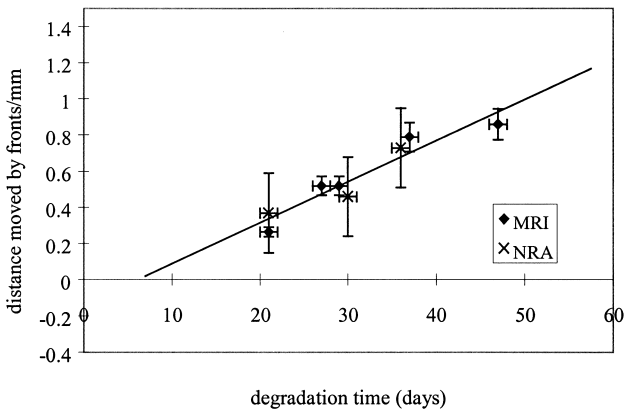


Fig. 11. A plot of distance moved by reaction–erosion fronts against degradation time determined from NRA and MRI.

The one-dimensional NRA data shown in Figs. 4 and 5 show data for PGA degradation in $D_2O/H_2O$ 50:50. The degradation occurred more quickly in $D_2O/H_2O$ 50:50 and $D_2O$ (Fig. 1) and this trend is seen in Figs. 4 and 5. These figures suggest that stage III started between 11 and 21 days and that the reaction–erosion fronts met between 45 and 57 days, earlier than the times recorded for the $D_2O$ data in Figs. 2 and 3. The results from Figs. 4 and 5 agree with the prediction made by Fig. 1 that little water is gained over the first 13 days and increase significantly afterwards at the start of stage III for PGA degradation in $D_2O/H_2O$ 50:50 PBS.

Fig. 6 compares one-dimensional NRA data for PGA degradation in $D_2O$ and $D_2O/H_2O$ 50:50 for similar time points. The data clearly show that at a given degradation time the levels of deuterium measured are higher in the samples degraded in $D_2O/H_2O$ 50:50. This result agrees with the information from Fig. 1 about the effect of deuterium on the rate of PGA degradation. The level of scatter in the data makes it difficult to compare the distance moved by the water fronts into the polymer from respective profiles.

In the early stages of degradation shown in Figs. 2 and 4, the shape of the concentration profiles appears Fickian in nature. This may be tested by fitting the data to the appropriate diffusion equation. In this way the bulk diffusion coefficient for water ingress before stage III may be calculated and compared with other values reported in the literature [19]. The diffusion coefficient is determined by using a solution to Fick's second law of diffusion [20].

$$\frac{\partial f(x,f)}{\partial t} = D\frac{\partial^2 f}{\partial x^2} \tag{2}$$

where $f$ is the water concentration, $x$ the distance, $D$ the diffusion coefficient and $t$ is the time.

The boundary conditions of the diffusing system determine which solution of Fick's second law is used. In this case, diffusion is occurring from an infinite supply of water into PGA disks, which are classed as a semi-infinite medium. The solution to Fick's second law for such a system is an error function, given below as:

$$f(x,t) = f_0 \operatorname{erf} c\left(\frac{x}{2\sqrt{Dt}}\right) \tag{3}$$

where $f_0$ is a constant.

This equation shows the water concentration decaying with $x$ at fixed $t$. Clearly, the decaying intensity observed at the edges of the samples as a result of any dehydration or chipping of the sample will introduce errors into values of $D$ obtained, but this approach still provides a useful rough guide.

Separate mean $D$ values are calculated from one-dimensional NRA profiles for hydration in $D_2O$ and $D_2O/H_2O$ 50:50 before stage III, at known times of $t$: for $D_2O$, these are the profiles for 1, 5 and 21 days, and for $D_2O/H_2O$, these are the profiles for 1, 3 and 11 days, presented, respectively in Figs. 2 and 4. Values of $f$ and $x$ are taken from parts of the one-dimensional NRA profiles that show apparent Fickian diffusion, and are fitted to a form of the error function (equation [3]) in Gnuplot, a UNIX-based data-fitting program. For some of the time points where the profiles are more smeared, only data from one side of the disk is used, but for others, the data from both sides are used. An average value of $D$, using all the appropriate individual $D$ values, is calculated for $D_2O$ and $D_2O/H_2O$ 50:50. Diffusion coefficient values are not calculated for later times, because it is not believed that diffusion in stage III is Fickian in nature. Figs. 7 and 8 show the fit of the NRA data for 3 days degradation in $D_2O/H_2O$ 50:50 and 5 days degradation in $D_2O$. Both show good agreement between the NRA data and the theoretical fit using the error function.

The mean diffusion coefficient calculated for hydration in $D_2O$ is $2.3 \times 10^{-13}$ m$^2$ s$^{-1}$ and for $D_2O/H_2O$ 50:50, is $1.3 \times 10^{-13}$ m$^2$ s$^{-1}$. The absolute error for both values is high at about $\pm 3 \times 10^{-14}$ m$^2$ s$^{-1}$, but despite this, the results more importantly indicate that both coefficient values are of $10^{-13}$ m$^2$ s$^{-1}$ in magnitude.

The diffusion coefficient values calculated for $D_2O$ and $D_2O/H_2O$ 50:50 are comparable to the diffusion coefficient of $5 \times 10^{-13}$ m$^2$ s$^{-1}$ ($\pm 1 \times 10^{-13}$ m$^2$ s$^{-1}$) determined by Zaikov et al., for bulk diffusion of water into PGA fibres [19]. It is worth noting that the diffusion coefficient values determined in this work apply to $D_2O$ diffusion, whereas, the coefficient value determined by Zaikov et al. applies to $H_2O$ diffusion. Literature reports the diffusion coefficients of $D_2O$ to be about 11% less than those for $H_2O$ [9]. This could account for some of the difference between our value and that reported by Zaikov et al. Further difference in the values might be caused by the different sample processing methods used in the respective studies (Zaikov et al., used PGA fibres, whereas, in this work, melt processed disks were used). In addition, the apparent smearing of the NRA one-dimensional profiles introduces inherent errors to the process of calculating a diffusion constant from the profile shape, which may also account for some of the difference.

The NRA results presented in this paper provide direct evidence about the hydration behaviour in PGA during stages I and II. The data show that during these two stages, water ingresses into the polymer at a low level, and in a Fickian manner, causing an inhomogeneous distribution in the water distribution. These interpretations are consistent with the four-stage model.

In thin samples, such as those made by Hurrell et al., which had thicknesses of approximately 0.5 mm, an equilibrium level of water was reached throughout the sample within a few hours, as a result of the kinetics of Fickian diffusion [1]. The point at which this diffusion was complete is defined as the end of stage I in the four stage model. In stage II in these samples, the water level remained approximately constant and uniform throughout the sample since Fickian diffusion was complete and the molecular weight at the surface has not fallen sufficiently for the creation of reaction–erosion fronts at the beginning of stage III. However, in thicker samples, such as the 2.3 mm thick samples used in these imaging experiments, the distances over which Fickian diffusion must take place are too large for the sample to have equilibrated before reaction–erosion fronts are set up at the surface. In these samples the distinction between stage I and stage II becomes more blurred. It could be argued that the samples progress directly from the Fickian diffusion of stage I to the reaction–erosion front movement of stage III without passing through the homogeneous water distribution state of stage II. It is interesting to note that the kinetics of reaction–erosion front movement did not appear to be much affected by changes in the sample thickness, even though the water content in the centre of the samples changed.

One and two-dimensional MRI data for PGA degradation in $D_2O/H_2O$ 50:50 are shown in Fig. 9 and may be compared with the NRA data shown in Figs. 4 and 5, which were collected under the same conditions of degradation. The earliest time point measured is 21 days. The data shows the fronts then progressed inwards for later time points from the sample surface until they met between 47 and 58 days. Afterwards, the water uptake continues, with water levels increasing by more in the centre than at the edges. The distribution was largely homogeneous by 75 days. In addition, the two-dimensional MRI images in Fig. 9 show that water fronts also ingressed from the sides of the disk during stage III at what appears to be the same rate as the fronts penetrating the top and bottom. The aspect ratio chosen for the samples meant that the water ingress from the sides of the disks made a small contribution to the bulk hydration of the polymer because the fronts had much further to travel before they meet in the centre than fronts penetrating from the top and bottom of the sample. The data extracted from the MRI images yielding one-dimensional profiles were selected from regions close to the centre of the images to ensure they corresponded to water ingress from the top and bottom of the disks.

Fig. 10 shows a good correlation between the integrated MRI profile signal intensity and the actual water gain measured gravimetrically. Both techniques show very little water gain occurred in polyglycolide during about the first 13 days of degradation (less than 1 wt%,), followed by more significant amounts taking place subsequently. This agrees with the degradation model. The agreement between the two sets of data (in the absence of full $T_1$ and $T_2$ corrections) offers very strong evidence that spatially resolved MRI data can give semi-quantitative information about the water levels in polyglycolide in this study.

The linear movement of the water fronts recorded during stage III by NRA and MRI does not obey the laws of Fickian

diffusion which would obey $t^{0.5}$ kinetics. In addition, although the kinetics of front movement in stage III share some similarities with Case II diffusion, differential scanning calorimetry (DSC) data from previous work suggested it was not an example of this type of diffusion either because polymer plasticisation occurred after a few hours of water penetration and not after several days, the time when reaction–erosion fronts are shown to start according to the imaging data [1].

The data shown in Figs. 4 and 5 for NRA and Fig. 9 for MRI can be compared. First, Fig. 1 predicted that the increased water uptake associated with the beginning of stage III occurred at about 13 days, and it can be argued that the data from both techniques are consistent with this. NRA data in Fig. 4 showed that significant water gain started between 11 and 21 days. The earliest time point which could be recorded by MRI was a few days after the start of stage III, at 21 days, also making the data consistent with the gravimetric data in Fig. 1.

Second, both sets of data show that water fronts progressed inwards from the sample surface towards the centre during stage III, the NRA images showing the $D_2O$ component and the MRI images the $H_2O$ component of the water fronts. This finding supports the hypothesis made by the degradation model that reaction–erosion fronts move from the sample surface towards the centre during this stage.

Finally, the techniques show the reaction–erosion fronts met at the same time (at the end of stage III) in a sample of thickness 2.3 mm. From the NRA data, this time point appears to have occurred between 45 and 57 days. The two-dimensional NRA image for 45 days appears to show the water fronts just before they meet, but these data have a high degree of scatter (because the sample used had undergone substantial cracking on cleavage) and so this interpretation of the data is not particularly conclusive. From the MRI data, the fronts appear to meet between 47 and 58 days, which overlaps well with the time range predicted by the NRA results.

These three pieces of evidence suggest that the data from the two techniques show the same hydration behaviour of PGA occurred during degradation in $D_2O/H_2O$ 50:50.

Further weight is added to this conclusion by plotting the distance moved by the water fronts into PGA disks against degradation time using the one-dimensional MRI and NRA profiles (Fig. 11). Despite the small number of data points, it is possible to conclude that, within experimental error, the two sets of data lie on top of each other. The *x*-intercept and gradient indicate that the reaction–erosion fronts begin at about 6($\pm$4) days, and move inwards from the surface to the centre of the sample at a rate of 0.023($\pm$0.003) mm/day.

On the strength of these discussions, it can be concluded that MRI and NRA gives the same information about a hydrating system containing both $H_2O$ and $D_2O$. It is believed that this is the first time a comparison has been demonstrated between the two techniques.

## 5. Conclusions

This section provides a summary of the conclusions drawn in Sections 3 and 4. MRI and NRA results provided direct evidence in support of the four-stage reaction–erosion model. Water gain and mass loss measurements showed that degradation proceeds more slowly with increasing amounts of deuterium but still involved a four-stage process. NRA, which detected deuterium concentrations in samples degraded in $D_2O$ and $D_2O/H_2O$ 50:50 buffers, showed that low levels of water penetrate the polymer in stage I through Fickian diffusion. The data also showed that hydration during stage III involved the movement of water fronts from the sample surface towards the centre. They met between 58 and 66 days in $D_2O$ and 45 and 57 days in $D_2O/H_2O$ 50:50. The information from the MRI data for $D_2O/H_2O$ 50:50 degraded samples agreed with the equivalent NRA data. Both predicted that the water fronts and hence the reaction–erosion fronts, begin at about 6($\pm$4) days, and move inwards from the surface to the centre of the sample at a rate of 0.023($\pm$0.003) mm/day.

## Acknowledgements

The authors are grateful to Pfizer Ltd and the EPSRC for financial support, Chris Burt for help with the Ion Beam Analysis equipment at the University of Surrey, and to Dr Susan Hurrell for help and advice.

## References

[1] Hurrell S, Cameron RE. J Mater Sci (Mater In Med) 2001;12:811.
[2] Vert M, Li SM, Garreau H. J Biomater Sci Polym Ed 1994; 6:639.
[3] Bell RP. The proton in chemistry. London: Chapman & Hall; 1973.
[4] Jenneson PM, Clough AS, Keddie JL, Lu JR, Meredith P. Nucl Inst Meth Phys Res B 1997; 132:697.
[5] Clough AS, Jenneson PM. Nucl Inst Meth Phys Res B 1998;139:51.
[6] Hollands R, Rutt H, Clough AS, Peel R, Smith R. Nucl Inst Meth Phys Res B 2001; 174:519–25.
[7] Riggs PD, Clough AS, Jenneson PM, Drew DW, Braden M, Patel MP. J Cont Rel 1999; 61:165–74.
[8] Tesmer JR, Nastasi M, editors. Handbook of modern ion beam analysis; Materials Research Society.
[9] Drew DW, Clough AS, Jenneson PM, Shearmur TE, van der Grinten MGD, Riggs P. Nucl Inst Meth Phys Res B 1996;119:429.
[10] Hyde T, Gladden L, Payne R. J Cont Rel 1995; 36:261.
[11] Dutheillet Y, Mantle M, Vesely D, Gladden L. J Polym Sci B 1999; 37:3328.
[12] Adriaensens P, Pollaris A, Carleer R, Vanderzande D, Gelan J, Litvinov VM, Tijssen J. Polymer 2001; 42(19):7943.
[13] Moerkerke R, Berghmans H, Vandeweerdt P, Adriaensen P, Ercken M, Vanderzande D, Gelan J. Macromol Chem Phys 2000;201(3): 308–12.
[14] Guiheneuf TM, Couzens PJ, Wille HJ, Hall LD. J Sci Food Agric 1997; 73(3):265–73.
[15] Callaghan PT. Principles of nuclear magnetic resonance microscopy. Oxford: Clarendon Press; 1991.

[16] Milroy GE, Mantle MD, Gladden LF, Huatan H, Cameron RE. J Mater Sci (Mater In Med) 2002; in press.
[17] Bostok L, Chandler S. Core maths for A-level. Cheltenham: Stanley Thornes; 1990.
[18] Milroy GE. PhD Thesis. University of Cambridge; 2001.
[19] Zaikov GE. J Mater Sci-Rev Macromol Chem Phys 1985; C25:551.
[20] Crank J. The mathematics of diffusion. Oxford: Clarendon Press; 1956.